Melanocyte Transformation Associated with Substrate Adhesion Impediment[1]

Sueli M. Oba-Shinjo[*,2], Mariangela Correa[†,2], Tatiana I. Ricca[†], Fernanda Molognoni[†], Maria A. Pinhal[‡], Izabel A. Neves[‡], Sueli K. Marie[*], Lúcia O. Sampaio[‡], Helena B. Nader[‡], Roger Chammas[§] and Miriam G. Jasiulionis[†]

*Laboratório de Biologia Molecular, Departamento de Neurologia, Faculdade de Medicina, Universidade de São Paulo, São Paulo, Brazil; †Disciplina de Imunologia, Departamento de Micro, Imuno e Parasitologia, Universidade Federal de São Paulo, São Paulo, Brazil; ‡Disciplina de Biologia Molecular, Departamento de Bioquímica, Universidade Federal de São Paulo, São Paulo, Brazil; §Laboratório de Oncologia Experimental, Faculdade de Medicina, Universidade de São Paulo, São Paulo, Brazil

Abstract

Exclude experimental models of malignant transformation employ chemical and physical carcinogens or genetic manipulations to study tumor progression. In this work, different melanoma cell lines were established after submitting a nontumorigenic melanocyte lineage (melan-a) to sequential cycles of forced anchorage impediment. The great majority of these cells underwent anoikis when maintained in suspension. After one deadhesion cycle, phenotypic alterations were noticeable in the few surviving cells, which became more numerous and showed progressive alterations after each adhesion impediment step. No significant differences in cell surface expression of integrins were detected, but a clear electrophoretic migration shift, compatible with an altered glycosylation pattern, was observed for β_1 chain in transformed cell lines. In parallel, a progressive enrichment of tri- and tetra-antennary N-glycans was apparent, suggesting increased *N*-acetylglucosaminyltransferase V activity. Alterations both in proteoglycan glycosylation pattern and core protein expression were detected during the transformation process. In conclusion, this model corroborates the role of adhesion state as a promoting agent in transformation process and demonstrates that cell adhesion disturbances may act as carcinogenic stimuli, at least for a nontumorigenic immortalized melanocyte lineage. These findings have intriguing implications for *in vivo* carcinogenesis, suggesting that anchorage independence may precede, and contribute to, neoplastic conversion.

Neoplasia (2006) **8,** 231–241

Introduction

The incidence of melanoma in most developed countries has increased more quickly than any other cancer type over the past 50 years [1]. Melanoma arises from the malignant transformation of pigment-producing cells (melanocytes), and this process results from complex interactions between genetic and environmental factors. Melanocytic nevi (moles), formed by benign clusters of melanocytes, have drawn special attention as potential precursor lesions, and "atypical nevi" are a marker for an increased risk of melanoma [2]. *In vivo*, 20% to 30% of human malignant melanomas are associated with benign or dysplastic nevi in histologic contiguity [3,4]. Clark et al. [5] proposed a five-stage model of melanoma progression from preneoplastic lesions (benign and dysplastic nevi) to thin radial growth superficial melanoma, followed by an invasive lesion and culminating in metastatic disease.

In humans, one of the first tissue alterations involved in melanoma progression is the presence of melanocytes in the dermis, topographically distant to basal keratinocytes. Keratinocytes in the "epidermal melanin unit" play a fundamental role in controlling the proliferation and expression of adhesion molecules in melanocytes, loss of cell–cell contact, and disruption of tissue architecture. Such activities have recently been implicated in genotypic and phenotypic changes in melanocytes [6].

The extracellular matrix (ECM) surrounding the cells is another important element controlling cell proliferation, adhesion, and migration. Changes in the expression or function of adhesion molecules, such as integrins, Mel-CAM/MUC18, CD44, intercellular adhesion molecule-1, cadherins, and cell surface

proteoglycans (PGs), have all been documented in the progression of primary melanomas [7,8]. In particular, the switch from a low-risk radial to a high-risk vertical growth primary melanoma is characterized by significant changes in the expression of molecules involved in cell–cell and cell–ECM contact, as well as of proteases [9].

Cell–ECM interactions have also been shown to determine the molecular progression of poorly metastatic melanoma cells, changing them to exhibit a highly aggressive phenotype [10]. The acquisition of resistance to cell death induced by substrate adhesion blockade (anoikis resistance) is a hallmark of neoplastic transformation and is also a critical step during metastatic progression [11].

Most findings relating adhesion molecules and the transformation process were obtained from primary skin cultures or human melanoma lesions in different stages of progression. Until now, all experimental models of melanocyte transformation utilize chemical or environmental carcinogens and genetic manipulations to study the progression of this deadly disease. In this work, we describe an *in vitro* murine model that focuses on cellular adhesion blockade as a transforming factor and characterize some alterations in adhesion molecule expression, which accompanies melanocyte transformation.

Materials and Methods

Cell Lines and Culture

The nontumorigenic murine melanocyte lineage, melan-a [12], a kind gift of Dr. Michel Rabinovitch (Department of Parasitology, UNIFESP, São Paulo, Brazil), was cultured in RPMI (pH 6.9; Gibco, Carlsbad, CA), supplemented with 5% fetal calf serum (Gibco) and 200 nM 12-*o*-tetradecanoyl phorbol-13-acetate (PMA; Tocris, Ellisville, MO) at 37°C in a humidified atmosphere of 5% CO_2 and 95% air. Melanoma cell lines (4C3, 4C8, 4C11, Tm1, Tm5, and S11) derived from melan-a cells after sequential cycles of substrate adhesion impediment were cultured in the same conditions, without PMA. Cell proliferation was determined using a standard methyl thiazol tetrazolium (MTT) assay [13].

Anchorage-Independent Growth Assays

The nontumorigenic cell line melan-a (10^5 cells/ml) was plated on 1% agarose and cultured for 96 hours in conditions described above. Small spheroids were collected by decantation and plated on standard culture plates, favoring cell adhesion. Cells were allowed to proliferate to subconfluent growth. The deadhesion (spheroid formation) cycle was repeated for four or five times; after the last deadhesion step, spheroids were counted and plated by limiting dilution (0.5–1 spheroid/well). Melan-a cells submitted to two and four deadhesion cycles were named, respectively, 2C and 4C. Tm1, Tm4, Tm5, S11, and 14 other melanoma cell lines were obtained by cloning melan-a cells submitted to five deadhesion cycles. In a second melan-a deadhesion assay, 4C3, 4C8, 4C11, and five other melanoma cell lines were established after four deadhesion steps.

Adhesion Assays

Briefly, 96-well microtiter plates were coated with 0.5 μg of human plasma fibronectin (Sigma, St. Louis, MO) or human placenta laminin (Calbiochem, San Diego, CA) in phosphate-buffered saline (PBS), incubated at 37°C for 2 hours, and blocked with 1% bovine serum albumin (BSA) for 1 hour after washing. Cells (3×10^4) suspended in 100 μl of serum-free RPMI were added to each coated well and incubated at 37°C for 30 minutes. Wells were washed three times with cold PBS to remove unbounded cells. Viable adherent cells were quantified using a standard MTT assay [13].

Immunofluorescence Microscopy

Different cell lines were cultured on glass coverslips until subconfluence and fixed in 1% paraformaldehyde in PBS. After washing with PBS, 50 mM glycine (pH 7.4) was added for 1 hour, and coverslips were blocked with 1% BSA. Cells were incubated for 1 hour with rabbit anti-fibronectin polyclonal antibody (Calbiochem), washed with 1% BSA, and incubated with an fluorescein isothiocyanate (FITC)–conjugated anti-rabbit antibody (KPL, Gaithersburg, MD) for 45 minutes. Slides were mounted and observed in a fluorescence microscope (Nikon Inc., Melville, NY).

Analysis of Surface Molecule Expression by Flow Cytometry

Expressions of integrins (α_v, α_5, α_6, β_1, and β_3 subunits) and leukoagglutinin from *Phaseolus vulgaris* (L-PHA)–positive glycoconjugates were quantified by flow cytometry. The cells were detached with trypsin, washed and suspended in PBS (1×10^6 cells/100 μl), and incubated with primary antibodies or FITC-conjugated L-PHA (Sigma; for L-PHA–positive glycoconjugates) on ice for 1 hour. All antibodies were diluted in PBS containing 0.5% BSA. The cells were then washed twice, suspended in 100 μl of appropriate FITC-conjugated anti-IgG on ice for 45 minutes, washed twice, and suspended in PBS. Negative controls were incubated only with secondary antibody. At least 10,000 cells were analyzed by Cell-QUEST program using FACSCalibur (Becton Dickinson Immunocytometry Systems, Franklin Lakes, NJ).

Western Blot Analysis and Lectin Blotting

Cells were washed twice with PBS and lysed in a buffer containing 1% Triton, 150 mM NaCl, 50 mM Tris HCl (pH 7.4), 5 mM EDTA, and protease and phosphatase inhibitors (0.5 mM phenylmethylsulfonyl fluoride, 10 μg/ml leupeptin, 10 μg/ml aprotinin, and 1 mM sodium orthovanadate) on ice for 15 minutes. The lysates were pelleted by centrifugation for 15 minutes at 4°C, and protein concentration was determined using the Bradford reagent (Bio-Rad, Hercules, CA). Equal amounts of protein (80 μg of total protein) from each sample were resolved by reduced 7.5% sodium dodecyl sulfate–polyacrylamide gel electrophoresis (SDS-PAGE) gels and blotted onto polyvinylidine fluoride membranes (Amersham, Piscataway, NJ). Membranes were blocked with 5% dried milk in PBS for 1 hour at room temperature before exposure to primary antibodies to β_1 integrin (rabbit polyclonal serum; a kind gift from Dr. K. Yamada, National Institute for Dental Research, Bethesda, MD) for 2 hours at

room temperature. Membranes were washed in 5% dried milk containing PBS and incubated with horseradish peroxidase (HPR)−conjugated anti-rabbit IgG (Sigma). After extensive washing with PBS, proteins were visualized by incubating the membrane with the substrate for peroxidase, diaminobenzidine (DAB; Sigma). For lectin blotting, after incubating the membrane with blocking reagent (Boehringer Mannheim, Mannheim), 1 μg/ml biotinylated L-PHA (Sigma) in blocking solution was added for 2 hours, followed by incubation with streptavidin HPR (R&D Systems, Minneapolis, MN) for another 1 hour at room temperature. The blots were washed and developed with DAB.

Tumorigenicity Assays

Cells were harvested after trypsin treatment of subconfluent monolayers, counted, and then suspended in PBS. Melan-a cells (2×10^7 cells) and its derived clones (1×10^6 cells) were injected subcutaneously in the flank of syngeneic 6- to 8-week-old C57Bl/6 female mice. Animals were kept under 12-hour daylight cycles, without food restriction, and checked daily for tumor development. Each experimental group consisted of at least five animals. Subcutaneous masses and axillary lymph nodes were excised and submitted to histologic analysis after paraffin embedding and hematoxylin and eosin (H&E) staining.

PG and Glycosaminoglycan (GAG) Analysis

Cell cultures were radiolabeled with 150 μCi of carrier-free ^{35}[S]sulfate (IPEN, São Paulo, Brazil) for 18 hours, essentially as previously described [14]. The medium was separated, and the cell layer and ECM were removed with 7 M urea in 12.5 mM Tris−HCl (pH 8.0). Each experiment was carried out in triplicate. For PG analysis, protease inhibitors were added to a final concentration of 100 mM α-aminocaproic acid, 6.5 mM benzamidine HCl, 5.5 mM iodoacetamide, and 0.1 mM phenylmethylsulfonyl fluoride. Total protein content was determined using the Bradford reagent and BSA as standard. For GAG analysis, 50 mM Tris−HCl buffer (pH 8.0), containing 0.15 M NaCl and 2 mg/ml maxatase (Biocon, Rio de Janeiro, Brazil), was added. The mixture was incubated at 50°C overnight and then at 100°C for 10 minutes to inactivate the protease. PG and sulfated glycosaminoglycan (SGAG)−free chains were analyzed by agarose gel electrophoresis in 50 mM 1,3-diaminopropane acetate buffer (pH 9.0), according to Nader et al. [15]. Electrophoresis was run for about 1 hour at 100 V, and compounds were precipitated in the gel with 0.1% CETAVLON (N-cetyl-N,N,N-trimethylammonium bromide) for at least 2 hours. The gel was dried and stained with 0.1% toluidine blue in 1% acetic acid and 50% ethanol. SGAG identification was based on the migration of the compounds, compared to standards, after exposure to X-ray film and degradation by specific enzymes [16]. Gel slices were cut and counted in scintillation liquid for the quantification of [^{35}S]sulfate-radiolabeled SGAG. Relative contents of disaccharides in chondroitin sulfate (CS) and dermatan sulfate (DS) were determined after incubation of SGAG (25,000 cpm) with chondroitinases AC (Tris−acetate 50 mM, pH 8.0) and ABC (ethylene diamine acetate buffer, EDA 0.05 M, pH 8.0) (Seikagaku, Tokyo, Japan). The relative amounts of disaccharides in heparan sulfate (HS) were determined after digestion of heparitinases I and II (0.05 M EDA, pH 7.0) [17,18]. Incubation mixtures were applied to descending paper chromatography [isobutyric acid: 1.25 M NH₄OH (5/3, vol/vol)]. Sulfated disaccharides were localized after exposure of the chromatogram to an X-ray film, cut, and counted in scintillation liquid.

Reverse Transcription Polymerase Chain Reaction (RT-PCR)

Total RNA were extracted from cultures with Trizol (Invitrogen, Carlsbad, CA), according to the manufacturer's instructions. One microgram of RNA was reverse-transcribed to cDNA with Superscript III (Invitrogen), according to the manufacturer's recommendations. PCR amplification was performed using the following primers: decorin (forward: 5′-gggtttggacaaagtgccctgg-3′; reverse: 5′-gcctggtgcatcaac-cttgg-3′; 512 bp), syndecan-4 (forward: 5′-tgctgctcctcggaggc-ttc-3′; reverse: 5′-ccttgggctctgaggggaca-3′; 282 bp), versican (forward: 5′-caaacccatgcctcaacggagg-3′; reverse: 5′-ccttca-gcagcatcccatgtgcgt-3′; 300 bp), perlecan (forward: 5′-gcccg-tgcacgctgagattga-3′; reverse: 5′-ggggcagaccctggatctaag-3′; 812 bp), heparanase (forward: 5′-ctcgagatgctgctgcgctcgaag-cctgcg-3′; reverse: 5′-ccatggtcaagtgcaagcagcaactttggc-3′; 1261 bp), and β-actin (forward: 5′-cttcgagcaggagatggcc-3′; reverse: 5′-ggtgcacgatggaggggccg-3′; 439 bp). Except for heparanase, the annealing temperature used in PCR amplification was 60°C, with different cycles. PCR reactions were performed in 25-μl reaction mixtures containing 75 mM Tris−HCl (pH 9.0), 2 mM MgCl₂, 50 mM KCl, 20 mM (NH₄)₂SO₄, 0.4 mM of each deoxynucleotide triphosphate, 0.4 μM of each primer, 1 U of BioTools DNA Polymerase—Recombinant from *Thermus thermophilus* (BioTools, Madrid, Spain), and 1 μl of cDNA in different dilutions. After the initial denaturing step for 5 minutes at 94°C, thermal cycling consisting of 35 cycles of 30 seconds, denaturing at 94°C, 30 seconds of annealing at 60°C, and 1 minute of extension at 72°C was carried out, followed by a final extension of 10 minutes at 72°C. For heparanase PCR, the reaction was performed using Master Mix Kit (Promega Biosciences Inc., Madison WI), 0.4 μM of each primer, 2 μl of cDNA, and 200 mM betaine. After a denaturing step at 94°C for 5 minutes, the following cycles were carried out: 5 cycles of 1 minute at 94°C, 1 minute at 60°C, and 2 minutes at 72°C; 20 cycles of 1 minute at 94°C, 1 minute at 55°C, and 2 minutes at 72°C; 10 cycles of 1 minute at 94°C, 1 minute at 50°C, and 2 minutes at 72°C; and a final extension step of 7 minutes at 72°C. PCR fragment amplification was confirmed by agarose gel staining with ethidium bromide.

Data Analysis

All experiments were repeated for at least two to three times with similar results. One-way analysis of variance (ANOVA) tests were used for most experiments, except where
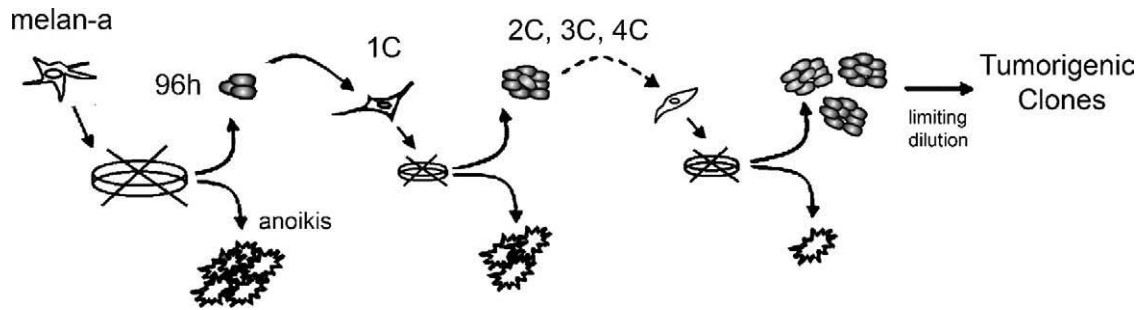
Figure 1. *Experimental model of melanocyte transformation induced by adhesion impediment. Schematic representation of the experimental protocol that resulted in melan-a transformation. After detachment from the substrate, surviving cells showed altered morphology and PMA-independent growth, even after one deadhesion cycle (1C).*

otherwise indicated. Statistical analysis was performed using GraphPad Prism 3.03 software (GraphPad, San Diego, CA).

Results

A New Model for Studying Melanocyte Transformation

A nontumorigenic murine melanocyte lineage, melan-a [12], was submitted to stressful conditions by blocking adhesion to substrate, as described above and as depicted in Figure 1. As expected for a nontumorigenic immortalized cell line, the great majority of these cells underwent apoptosis induced by adhesion blockade (anoikis). After cultivating melan-a cells in agarose-coated plates for 96 hours, only 10^3 small spheroids per 10^6 plated cells were observed. Each spheroid is probably derived from a single cell, thus suggesting that only 0.1% of the initial cell number was able to resist anoikis (Table 1).

Anoikis-resistant melan-a cells were cultured in adherent conditions and submitted to new deadhesion cycles. Surviving melan-a cells submitted to two, three, and four deadhesion cycles were kept in adherent conditions and designated 2C, 3C, and 4C, respectively. Distinct lineages (4C3, 4C8, 4C11, S11, Tm1, Tm4, Tm5, and others) were obtained by limiting dilution after a new deadhesion cycle of 4C cells (0.5 spheroid/well) (Figure 1).

Altered morphology was observed in all melan-a−derived cell lines (including 1C to 4C cells), which demonstrated stable phenotypic characteristics and melanin production (data not shown). Although melan-a cells require PMA as a growth factor, all these lineages showed PMA-independent growth, as described for human melanoma cell lines [19]. Furthermore, cell lines obtained after submitting melan-a cells to adhesion impediment cycles showed increased spheroid formation and shorter doubling times compared to the original melan-a cells (Table 1). Immunofluorescence analysis using a specific antibody showed that melan-a−derived sublines Tm1 and Tm5 did not assemble fibronectin on the ECM, unlike melan-a cells (Figure 2A). Curiously, tested cell lines obtained after four or five deadhesion steps and after limiting dilution (4C11, Tm1 and Tm5) showed higher adhesiveness both to fibronectin (Figure 2B) and laminin (Figure 2C).

Considering several phenotypic characteristics associated with neoplastic transformation that were observed in melan-a−derived cell lines, *in vivo* tumorigenic capacity was tested. Surprisingly, all lineages obtained after four deadhesion cycles were able to grow as tumors when injected subcutaneously in syngeneic mice (Figure 2D), with different latency times for tumor appearance (Table 1). In the first melan-a detachment assay, we obtained 16 different cell lines; 12 were injected in the subcutaneous tissue and every one of them resulted in palpable tumors (from 5 to 20 mm in diameter) in all injected animals (groups of three to five animals). Subcutaneous tumors derived from seven cell lines (Tm1, Tm4, Tm5, S10, S11, a1, and a3) were submitted to histologic analysis, and all showed cytologic and histologic characteristics of malignant cells. All cell lines, except Tm1 and a1, showed a melanotic appearance at microscopy. In the second assay, eight cell lines were obtained. Four of them (4C1, 4C3, 4C8, and 4C11) were injected into syngeneic mice, and all resulted in subcutaneous tumors when injected subcutaneouly.

When 10^6 cells were transplanted subcutaneouly into animals, the amelanotic Tm1 and melanotic Tm5 cell lines showed very short latency times for tumor appearance (up to 10 days) compared to 4C3, 4C8, and 4C11 (at least 30 days). Spontaneous lymph node metastases were identified in animals injected subcutaneouly with 10^6 Tm1, Tm4,

Table 1. Some Phenotypic Alterations of Melan-A−Derived Lineages.

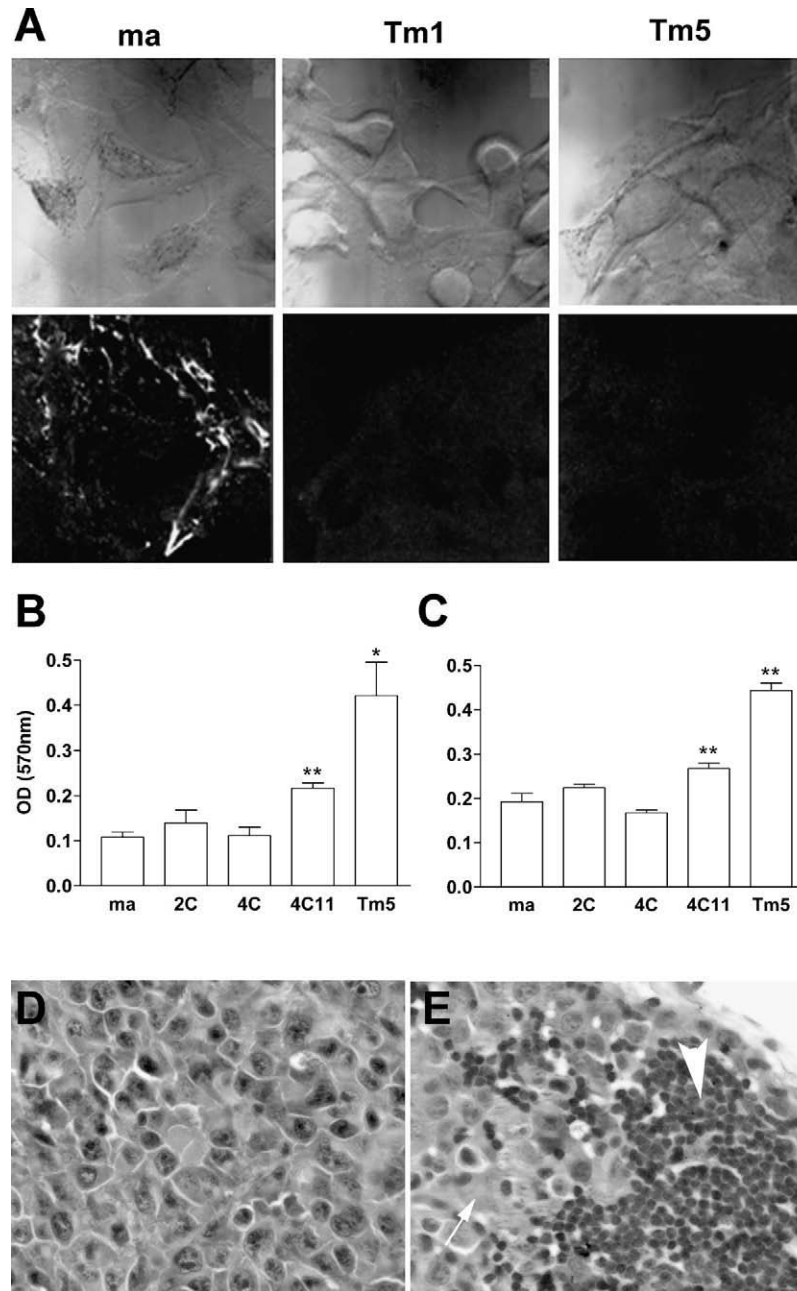| Cell Lines	Spheroid Formation (%)*	Melanin Production	Latency In Vivo[†] (days)	Doubling Time In Vitro (hours)
Melan-a	0.1	+	Nontumorigenic	22
2C	ND	+	Nontumorigenic	22
4C	ND	+	Nontumorigenic	20
4C3	ND	−	>33	ND
4C11	ND	−	>33	ND
S11	10	+	<14	ND
Tm1	25	−	<10	18
Tm5	32	+	<9	14

ND, not done.
*Number of spheroids formed after plating 10^6 cells in suspension.
[†]Tumorigenicity of cells injected subcutaneously in the flanks of C57Bl/6 mice (1 million cells per flank).

Figure 2. *Morphologic and functional characteristics of melan-a–derived cell lines. (A) Phase-contrast microscopy (upper panels) and indirect immuno-fluorescence depicting fibronectin deposition on ECM by melan-a, Tm1, and Tm5 cells, using a specific polyclonal antibody against fibronectin (lower panels). Adherent cell number, as measured by an MTT protocol, after plating cells for 30 minutes in fibronectin-coated (B) or laminin-coated (C) wells. Paired t test was used for statistical comparisons between melan-a cells and derived lineages (*P < .05, **P ≤ .01). Histologic analysis of tumor masses (D) and axillary lymph nodes (E) obtained from syngeneic mice injected with 10^6 cells, 14 days after injection. The large arrow indicates axillary lymph node, and the small arrow shows infiltrating melanoma cells. H&E staining, ×40.*

and Tm5 melanoma cells (Figure 2*E*), but not with 4C3, 4C8, or 4C11. Tm1, Tm4, and Tm5 showed *in vivo* characteristics of an aggressive phenotype, whereas 4C3, 4C8, and 4C11 were considered indolent melanoma lineages.

Conversely, direct cloning of melan-a cells (not submitted to the deadhesion protocol) did not render tumorigenic lineages (data not shown). Melan-a cells have never been shown to be tumorigenic, even when a great number of cells (2×10^7 cells/animal) were transplanted subcutaneouly into mice and observed for at least 80 days.

Melanoma Cells Derived from Melan-A Showed Significant Alterations in Glycoconjugates

Because malignant phenotype was acquired after repetitive cycles of adhesion blockade, adhesion molecule expression was investigated. Integrins are an important family of adhesion molecules involved both in cell–cell and cell–ECM interactions, and alterations in their expression and/or processing are frequent in several types of malignancies [20]. Surface expression of β_1, β_3, α_5, α_6, and α_v integrin chains was determined by flow cytometry using specific antibodies,

and no substantial differences were found in their surface expression levels (data not shown). Although we could not detect differences on β_1 integrin surface expression, Western blot analysis revealed that melan-a–derived melanomas (Tm1 and Tm5) have a β_1-chain with a different migration pattern on SDS-PAGE when compared to melan-a cells (Figure 3D), suggesting a posttranslational processing of β_1 integrins. The same altered electrophoresis mobility was observed for the β_1 integrin chain of a well-known murine melanoma cell line B16F10.

As previously shown by our group and others [21], a similar shift of β_1 integrin chain migration pattern is observed in several tumor types and is commonly related to aberrant glycosylation resulting from N-acetylglucosaminyltransferase V (GnT-V) enzymatic activity. Tri-antennary or tetra-antennary oligosaccharides formed by this enzyme activity are recognized by L-PHA, and, as seen in Figure 3, A and B, melan-a–derived melanomas show a higher expression of L-PHA–positive surface glycoconjugates compared to their parental cell line. Interestingly, cell lineages obtained after submitting melan-a to two or four deadhesion cycles (2C and

4C cell lines) already demonstrate a slightly higher L-PHA–binding glycoconjugate expression compared to melan-a. The total glycoprotein profile, shown by lectin blotting on Figure 3C, detailed qualitative and quantitative alterations observed after melan-a transformation.

Another important class of glycoconjugates comprises ECM and surface PGs, which have complex structures, with a protein core bearing at least one GAG chain. GAGs are involved in cell growth, cell migration, and cell–cell and cell–matrix interactions—phenomena that are essential for tumor development. Initial analysis revealed important modifications in electrophoretic PG profiles, both from cell surface and culture supernatant extracts (data not shown). These results led us to investigate the GAG composition of these glycoconjugates.

Melanoma Cells Present an Altered GAG Profile Compared to That of Melan-A Melanocytes

We analyzed GAG chains from cells and culture supernatants from melan-a, Tm1, Tm5, and S11 cells (Figure 4A). Melan-a has a tendency to accumulate PGs bearing HS on
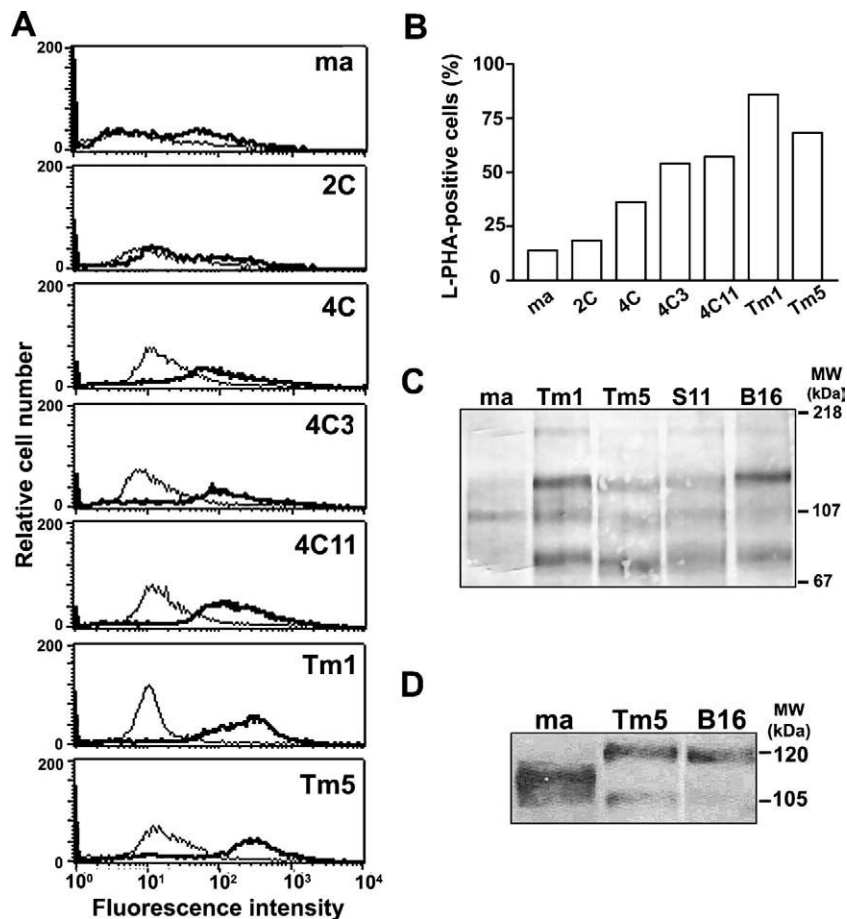
Figure 3. Melan-a transformation is accompanied by an increase in tri-antennary and tetra-antennary oligosaccharides and by modification in β_1 integrin chain. (A) Cell surface tri-antennary and tetra-antennary oligosaccharide expression on melan-a (ma), 2C, 4C, 4C3, 4C11, Tm1, and Tm5 cell surfaces analyzed by flow cytometry using biotin–L-PHA lectin and FITC–streptavidin. (B) Proportion of L-PHA–positive cells (same experiment as in A) (C). Glycoproteins from cell extracts containing tri-antennary and tetra-antennary N-glycans, as shown by lectin blotting using L-PHA lectin. Analysis by flow cytometry of tri-antennary and tetra-antennary oligosaccharide expression, as recognized by L-PHA lectin (D). β_1 integrin expression on melan-a (ma), Tm5, and B16F10 cells visualized by Western blot analysis, using a specific polyclonal antibody.
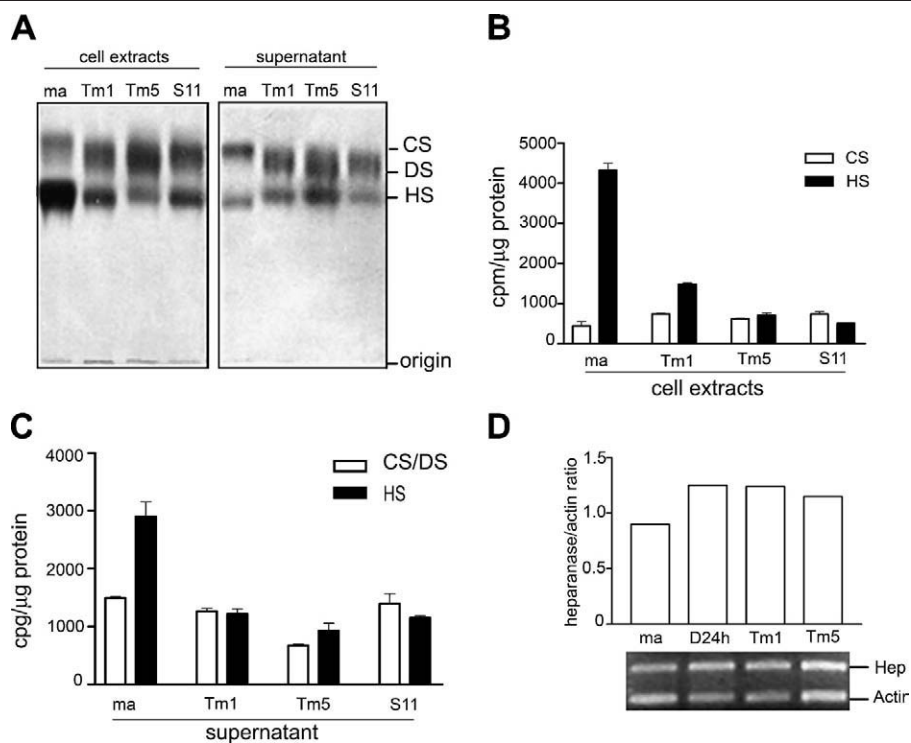
Figure 4. Melanoma cell lines show a band shift of CS toward DS and decreased levels of HS. (A) GAGs from cellular extracts and culture supernatants of melan-a (ma) and derived melanoma cell lines (Tm1, Tm5, S11). (B and C) [^{35}S]sulfate incorporation in CS/DS and HS chains. Total amount of [^{35}S] incorporated in each SGAG was determined by cutting radioactive bands from gel slides, counting in scintillation liquid, and normalizing for the protein content (cpm/μg protein) of cell extracts (B) and culture supernatants (C). (D) Heparanase mRNA expression (Hep) in melan-a (ma), melan-a maintained in suspension for 24 hours (D24 h), and Tm1 and Tm5 melanoma cells. CS, chondroitin sulfate; DS, dermatan sulfate; HS, heparan sulfate.

the cell surface and/or ECM, whereas tumorigenic melanoma cell lines tend to express both HS and CS/DS PGs. There is a clear difference in the electrophoretic migration of CS synthesized by melan-a and its derived melanoma cell lines. A band shift toward standard DS suggested an increase in the amounts of iduronic acid–containing disaccharides in the galactosaminoglycans of tumorigenic sublines. The amount of [^{35}S]GAG in relation to total protein content was determined for HS and CS/DS, showing a significant decrease of HS chains in cell extracts (Figure 4B) and supernatants (Figure 4C) from tumorigenic cell lines, compared to those from melan-a cells. Such decrease in the incorporation of sulfate into HS could reflect a decrease in synthesis (sulfation) and/or an increase of chain degradation. In our model, this HS reduction can be explained by a progressive increase in heparanase expression along the melan-a transformation process, as depicted in Figure 4D. Heparanase is involved in the degradation of both cell surface and ECM HS chains [22], and elevated expression of this enzyme has been associated with tumor development and metastasis [23–25] In addition, HS disaccharide composition was very similar in melan-a and in its derived sublines, except for the Tm1 melanoma cell line. HS from Tm1 showed a decrease in the disaccharide bearing 2-O-sulfate in the uronic acid residue in relation to parental melanocytes (Table 2).

The sulfated disaccharide composition for both secreted and cellular CS/DS from each cell type was determined after digestion with chondroitinases AC and ABC (Table 3). There is a clear difference in the ratio of glucuronic acid– and

iduronic acid–containing disaccharides obtained by the degradation of galactosaminoglycans when comparing parental melanocyte lineage and its derived tumorigenic melanoma cell line. Melan-a cells had mainly galactosaminoglycan chains enriched in glucuronic acid–containing disaccharides, whereas in tumorigenic counterparts, an important increase in the relative amounts of iduronic acid–containing disaccharides was observed. Furthermore, the CS/DS chains of the tumorigenic cells also showed 6-sulfated disaccharides, which were not detected in the parental cell line.

Table 2. Relative Proportion of Heparan [^{35}S]Sulfate Disaccharides Yielded by Degradation with Heparitinases I and II.

HS	Supernatants				Cell Extracts			
	ma	Tm1	Tm5	S11	ma	Tm1	Tm5	S11
ΔUA-GlcNAc,6S	11	10	10	11	9	9	8	10
ΔUA-GlcNS	41	37	34	36	33	33	25	31
ΔUA-GlcNS,6S	29	43	41	35	36	44	44	35
ΔUA,2S-GlcNS,6S	19	11	15	18	22	14	23	24

The radioactivity of the disaccharides was measured after the separation (by paper chromatography) of compounds incubated with both heparitinases I and II. The types of uronic acid were not taken into account.
ma, melan-a; Tm1, Tm5, and S11, tumorigenic melanoma cell lines; ΔUA-GlcNS, O-(4-deoxy-hex-4-enopyranosyluronic acid)-(1–4)-2-sulfamino-ᴅ-glucose; ΔUA-GlcNAc,6S, O-(4-deoxy-hex-4-enopyranosyluronic acid)-(1–4)-2-acetamido-ᴅ-glucose 6-sulfate; ΔUA-GlcNS,6S, O-(4-deoxy-hex-4 enopyranosyluronic acid)-(1–4)-2-sulfamino-ᴅ-glucose 6-sulfate; ΔUA,2S-GlcNS,6S, O-(4-deoxy-hex-4-enopyranosyluronic acid 2-sulfate)-(1–4)-2-sulfamino-ᴅ-glucose.

Table 3. Relative Proportion of Chondroitin [^{35}S]Sulfate/Dermatan [^{35}S]Sulfate Disaccharides Yielded by Degradation with Chondroitinases AC and ABC.

CS/DS	Supernatants				Cell Extracts			
	ma	Tm1	Tm5	S11	ma	Tm1	Tm5	S11
ΔIdoA-GalNAc,4S	0	23	30	20	22	9	26	30
ΔGlcA-GalNAc,4S	100	57	46	57	78	76	50	57
ΔGlcA-GalNAc,6S	0	20	24	23	0	15	24	13

The radioactivity of the disaccharides was measured after separation by paper chromatography. Chondroitinase AC exclusively yields glucuronic acid–containing disaccharides, whereas chondroitinase ABC yields both glucuronic acid– and iduronic acid–containing disaccharides. The relative amount of ΔIdoA-4S was obtained by the difference between degradation product yields after the action of both chondroitinases.

ma, melan-a; Tm1, Tm5, and S11, tumorigenic melanoma cell lines; ΔIdoA-GalNAc,4S, O-(4-deoxy-hex-4-enopyranosyluronic acid)-(1–3)-2-acetamido-D-galactose 4-sulfate; ΔGlcA-GalNAc,4S, O-(4-deoxy-hex-4-enopyranosyluronic acid)-(1–3)-2-acetamido-D-galactose 4-sulfate; ΔGlcA-GalNAc,6S, O-(4-deoxy-hex-4-enopyranosyluronic acid)-(1–3)-2-acetamido-D-galactose 6-sulfate.

Melanocyte Transformation Is Accompanied by Alterations in Decorin, Versican, and Perlecan Expressions

To better characterize PG expression alterations that occur during melanocyte transformation induced by cycles of substrate adhesion blockade, we analyzed protein core expression by semiquantitative RT-PCR (Figure 5). We also analyzed melan-a cells submitted to two and four deadhesion cycles (2C and 4C cell lines) and two other melanoma cell lines (4C3 and 4C8) for protein core transcripts. Perlecan, versican, and decorin (but not syndecan- 4) protein core expressions were altered in melanoma cell lines, compared to those in melan-a and 2C cells. Interestingly, nontumorigenic 2C and 4C cell lines, submitted to two and four deadhesion cycles, already showed some of these modifications, suggesting that these PGs are associated with melanocyte transformation in our model.

Discussion

Acquisition of anchorage-independent growth is a hallmark of neoplastic transformation, but this property is not considered to be carcinogenic per se. In this work, we show that repetitive adhesion blockade events are sufficient to induce malignant transformation in nontumorigenic immortalized melanocytes (melan-a). Although we cannot exclude clonal selection as the principal mechanism responsible for tumorigenic conversion, several results indicate that adhesion impediment may trigger the carcinogenic process. All tumorigenic cell lines derived from melan-a have faster doubling times than their parental lineage (Table 1), but even after 80 *in vitro* passages, melan-a cells were never tumorigenic *in vivo* (data not shown). No negative influence of melan-a over its derived subline proliferation rate could be demonstrated either *in vitro* (not shown) or *in vivo* [26]. In addition, cell clones obtained after limiting the dilution of melan-a cells
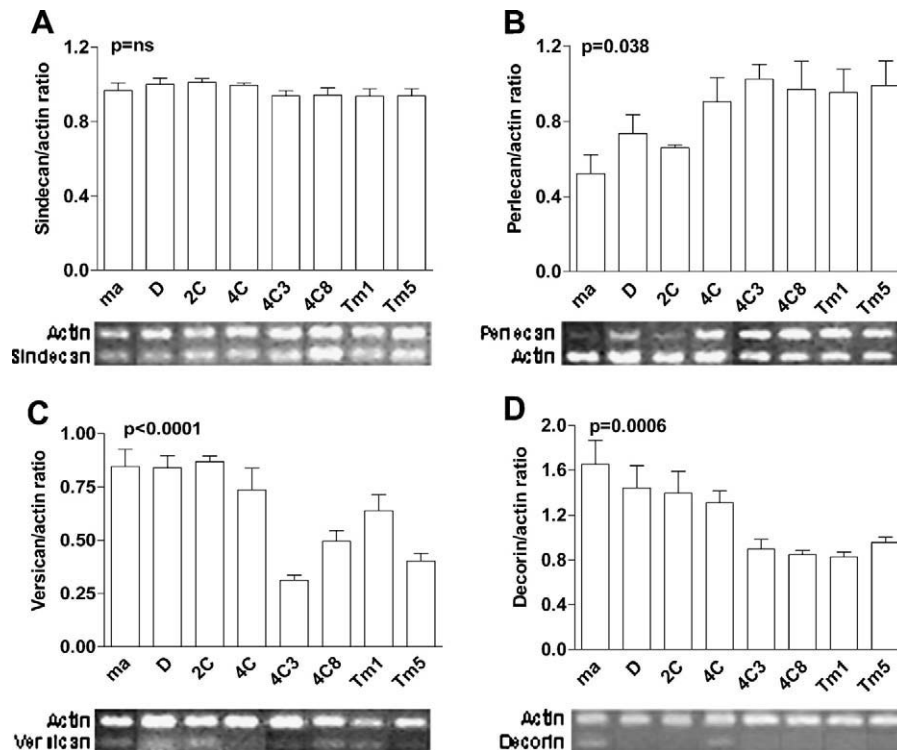
Figure 5. *The expression of perlecan, versican, and decorin, but not syndecan-4, becomes altered during melan-a transformation. cDNA obtained from RT was diluted and amplified by semiquantitative PCR for syndecan-4 (A), perlecan (B), versican (C), and decorin (D), with resulting products visualized on agarose gel. Ethidium bromide staining intensity was analyzed for each gene and for an internal control (β-actin). Numbers on the y axis represent the mean ratio between protein core/β-actin expression for each cell type, determined for four different cDNA dilutions. Amplified products from one initial cDNA dilution are depicted below each panel for syndecan-4 (1:16), perlecan (1:16), versican (1:8), decorin (1:2), and β-actin (same dilution as that of the respective protein core). ma, melan-a; D, melan-a submitted to adhesion blockade for 24 hours. ANOVA tests[35] were used for statistical analysis.*

were not tumorigenic *in vivo*, suggesting that transformed cells are not initially present in the parental cell line (not shown) and that repeated adhesion blockade is important to induce malignant phenotype. Epigenetic modifications are the most probable candidates to explain the myriad of morphologic and molecular alterations observed after repeated deadhesion cycles, and preliminary results from ongoing experiments in our laboratory indicate that such is the case, indeed.

Stressful conditions resulting from cell–cell and cell–substrate adhesion modifications have previously been associated with malignant transformation. Rubin [27] has consistently shown that high-density cultures yield tumorigenic clones, which he attributes to clonal selection, without excluding a direct effect of adhesion alterations in the carcinogenic process. Another group has shown that the forced anchorage-independent growth of a nontumorigenic, immortalized epithelial cell line resulted in the acquisition of an anoikis-resistant phenotype and in tumorigenesis [28]. As demonstrated by Zhu et al. [29], selected anoikis-resistant melanoma cells showed increased metastatic potential and multiple alterations in their phenotypic properties. Diaz-Montero and McIntyre [30] obtained anoikis resistance osteosarcoma sublines through modifications of culture conditions, attributing this phenotype to epigenetic events. Ongoing research in our laboratory has shown that adhesion alterations can also induce malignant transformation in the fibroblast cell line NIH 3T3, implying adhesion loss as a crucial factor for carcinogenesis in different cell types.

Interestingly, the proportion of spheroid formation for each cell line (melan-a and derived lineages; Table 1) resembles the percentage of soft agar cell growth from different phases of melanocyte transformation [31], where melan-a corresponds to dysplastic lesions and Tm melanoma cells correspond to invasive melanoma. These results reinforce the idea that the cell lines utilized in this work truly represent a continuum along the transformation process.

Integrins, which are the most important class of adhesion molecules related to ECM interactions, have been shown in most cellular types to impart survival signals on adhesion to substrate and surface clustering [32,33]. However, Lewis et al. [34] showed that loss of integrin-mediated cell adhesion may abrogate cell death in cells submitted to DNA damage, through p19^{Arf} and p53 signaling. In melan-a–derived cell lines, no modification of β_1, β_3, α_5, α_6, and α_v integrin expression was detected (not shown). Nevertheless, an electrophoretic migration shift was observed for β_1 integrin chain (Figure 3D), which has been demonstrated by several groups, including ours, to be related to an aberrant N-glycosylation pattern [35,36]. This alteration, caused by GnT-V overexpression, is associated with acquisition of migratory phenotype and tumor progression [37]. The forced expression of GnT-V results in decreased fibronectin attachment of colon carcinoma cells [38] possibly caused by aberrant β_1 integrin chain glycosylation [35], but this same, the glycosylation pattern was associated with increased fibronectin adhesion (Figure 2B) in the melanoma cell lines presented here.

Although GnT-V expression was not investigated, a marked increase of its products (GlcNAcβ1,6Manα1,6–branched surface molecules) was demonstrated for all melan-a–derived cell lines in a progressive manner during the transformation process (Figure 3, A and B). A qualitative alteration in the N-glycosylation protein profile was demonstrated for melanoma cells derived from melan-a (Figure 3C). The above studies and our findings suggest that GnT-V activity is causally associated with malignant transformation because melan-a cells submitted to sequential deadhesion cycles (but not yet tumorigenic) already show augmented levels of tri-antennary and tetra-antennary N-glycan products.

Even though it is quite clear that several tumors accumulate glycoproteins bearing β1–6–branched N-linked oligosaccharides recognized by L-PHA, the precise function of this altered pattern of glycosylation in glycoprotein function remains elusive. An interesting hypothesis considering GnT-V as a transforming enzyme was proposed by Dennis et al. [39], who had initially shown that its forced expression in a nontumorigenic cell line could convert those cells capable of forming tumors in nude mice [40]. Based on more recent studies, Morgan et al. [41] proposed that growth factor and cytokine receptors, which are also modified by GnT-V, exist as lattices on the cell surface. Maintenance of these lattices would depend on extracellular glycan-binding proteins, such as galectins. Complexes of glycoproteins and lectins would render cells more sensitive to growth factors, whose interaction with their cognate receptors usually lead to receptor dimerization/oligomerization. If correct, the prediction is that L-PHA binding correlates with autonomous growth. Integrins [35,42,43] and cadherins [44,45] are also substrates of GnT-V. Similarly to integrins, no differences in cadherin expression were detected by serial analysis of gene expression [46], RT-PCR, or Western blot analysis (data not shown). The higher adhesiveness of tumorigenic cell lines (4C11 and Tm5), both to fibronectin and laminin (Figure 2, B and C), could be attributed to this aberrant glycosylation pattern present in β_1 integrin chains. However, the true impact of this pattern of glycosylation in this model warrants further investigation.

PGs, another class of surface molecules, are also involved in neoplastic transformation in several cell types. HS and CS have been particularly implicated in tumor formation, including melanoma, because of their capacity to bind and modulate a large number of molecules that are important for tumor development, such as basic fibroblast growth factor and vascular endothelial growth factor [47]. HS may either promote or inhibit tumor progression, depending on heparan fragments generated on digestion [48]. In our model, the expression of HS was significantly decreased after transformation, although no structural modifications were discernible (Figure 4; Table 2). In parallel, an increased expression of heparanase was demonstrated not only in melan-a–derived melanoma cell lines, but also in melan-a maintained in suspension for 24 hours, indicating that heparanase may contribute to early changes involved in melan-a transformation. Using a different approach for the detection of heparanase

in different melanoma cell lines, an increase in enzymatic activity was related to a higher metastatic phenotype [49]. However, CS/DS levels were similar in both nontumorigenic and tumorigenic cell lines, but their disaccharide composition was clearly different from the parental cell lineage (Figure 4; Table 3). It is clear that transformation leads to an increase in the relative amounts of α-L-iduronic acid, suggesting a possible upregulation of the β-D-glucuronic acid C-5-epimerase. Furthermore, during transformation, the glucuronic acid–containing disaccharides show the presence of N-acetylgalactosamine-6-O-sulfate, contrasting with the parental line that bears only N-acetylgalactosamine-4-O-sulfate, indicating that malignant transformation leads to the expression of N-acetylgalactosamine 6-O-sulfotransferase, as previously observed in brain tumors [50].

In addition, the protein core expression levels of some PG subclasses were determined by semiquantitative RT-PCR. As shown in Figure 5, perlecan levels increase during transformation, decorin and versican levels decrease, and syndecan-4 level does not change. Among extracellular PGs, decorin has emerged as an inhibitor of tumor progression, whereas perlecan seems to be a promoter of this process [51,52]. Perlecan apparently supports the growth and invasion of tumor cells through its ability to store angiogenic factors [53]. This last observation also corroborates our hypothesis that melan-a–derived melanoma cell lines were not selected by multiple cycles of adhesion blockade because perlecan increased during the transformation process even in the absence of a selective pressure related to angiogenesis.

Our model of melanocyte carcinogenesis allows the identification of morphologic and molecular alterations that precede full malignant transformation and reinforce microenvironmental role as a transforming factor, particularly the loss of cell–substrate adhesion.

References

[1] Oliveria S, Dusza S, and Berwick M (2001). Issues in the epidemiology of melanoma. *Expert Rev Anticancer Ther* **1,** 453–459.

[2] Houghton AN and Polsky D (2002). Focus on melanoma. *Cancer Cell* **2,** 275–278.

[3] Elder DE, Greene MH, Bond EE, and Clark WH (1981). Acquired melanocytic nevi and melanoma: the dysplastic nevis syndrome. In Ackerman, AB (Ed), *Pathology of Malignant Melanoma*. New York: Masson, pp. 185–215.

[4] Gruber SB, Barnhill RL, Stenn KS, and Roush GC (1989). Nevomelanocytic proliferations in association with cutaneous malignant melanoma: a multivariate analysis. *J Am Acad Dermatol* **21,** 733–780.

[5] Clark WH Jr, Elder DE, Guerry D IV, Epstein MN, Greene MH, and Van Horn M (1984). A study of tumor progression: the precursor lesions of superficial spreading and nodular melanoma. *Hum Pathol* **15** (12), 1147–1165.

[6] Hsu MY, Meier FE, Nesbit M, Hsu JY, Van Belle P, Elder DE, and Herlyn M (2000). E-cadherin expression in melanoma cells restores keratinocyte-mediated growth control and down-regulates expression of invasion-related adhesion receptors. *Am J Pathol* **156** (5), 1515–1525.

[7] Bogenrieder T and Herlyn M (2002). Cell-surface proteolysis, growth factor activation and intercellular communication in the progression of melanoma. *Crit Rev Oncol Hematol* **44,** 1–15.

[8] Li G, Satyamoorthy K, and Herlyn M (2002). Dynamics of cell interactions and communications during melanoma development. *Crit Rev Oral Biol Med* **13,** 62–70.

[9] Herlyn M, Padarathsingh M, Chin L, Hendrix M, Becker D, Nelson M, DeClerck Y, McCarthy J, and Mohla S (2002). New approaches to the biology of melanoma: a workshop of the National Institutes of Health Pathology B Study Section. *Am J Pathol* **161** (5), 1949–1957.

[10] Hendrix MJ, Seftor EA, Kirschmann DA, Quaranta V, and Seftor RE (2003). Remodeling of the microenvironment by aggressive melanoma tumor cells. *Ann NY Acad Sci* **995,** 151–161.

[11] Grossmann J (2002). Molecular mechanisms of "detachment-induced apoptosis—Anoikis". *Apoptosis* **7,** 247–260.

[12] Bennett DC, Cooper PJ, and Hart IR (1987). A line of non-tumorigenic mouse melanocytes, syngeneic with the B16 melanoma and requiring a tumour promoter for growth. *Int J Cancer* **39,** 414–418.

[13] Mosmann T (1983). Rapid colorimetric assay for growth and survival: application to proliferation and cytotoxicity assays. *J Immunol Methods* **65,** 55–63.

[14] Porcionatto MA, Moreira CR, Lotfi CF, Armelin HA, Dietrich CP, and Nader HB (1998). Stimulation of heparan sulfate proteoglycan synthesis and secretion during G1 phase induced by growth factors and PMA. *J Cell Biochem* **70** (4), 563–572.

[15] Nader HB, Dietrich CP, Buonassisi V, and Colburn P (1987). Heparin sequences in the heparan sulfate chains of an endothelial cell proteoglycan. *Proc Natl Acad Sci USA* **84,** 3565–3569.

[16] Nader HB, Buonassisi V, Colburn P, and Dietrich CP (1989). Heparin stimulates the synthesis and modifies the sulfation pattern of heparan sulfate proteoglycan from endothelial cells. *J Cell Physiol* **140,** 305–310.

[17] Nader HB, Porcionatto MA, Tersariol IL, Pinhal MA, Oliveira FW, Moraes CT, and Dietrich CP (1990). Purification and substrate specificity of heparitinase I and heparitinase II from *Flavobacterium heparinum*. Analyses of the heparin and heparan sulfate degradation products by ^{13}C NMR spectroscopy. *J Biol Chem* **265,** 16807–16813.

[18] Nader HB, Kobayashi EY, Chavante SF, Tersariol IL, Castro RA, Shinjo SK, Naggi A, Torri G, Casu B, and Dietrich CP (1999). New insights on the specificity of heparin and heparan sulfate lyases from *Flavobacterium heparinum* revealed by the use of synthetic derivatives of K5 polysaccharide from *E. coli* and 2-O-desulfated heparin. *Glycoconj J* **16,** 265–270.

[19] Mufson RA, Fisher PB, and Weinstein IB (1979). Effect of phorbol ester tumor promoters on the expression of melanogenesis in B-16 melanoma cells. *Cancer Res* **39** (10), 3915–3919.

[20] Hynes RO (2002). Integrins: bidirectional, allosteric signaling machines. *Cell* **110,** 673–687.

[21] Gu J and Taniguchi N (2004). Regulation of integrin functions by N-glycans. *Glycoconj J* **21,** 9–15.

[22] Cohen IR, Murdoch AD, Naso MF, Marchetti D, Berd D, and Iozzo RV (1994). Abnormal expression of perlecan proteoglycan in metastatic melanomas. *Cancer Res* **54,** 5771–5774.

[23] Hullet MD, Freeman C, Hamdorf BJ, Baker RT, Harris MJ, and Parish CR (1999). Cloning of mammalian heparanase, an important enzyme in tumor invasion metastasis. *Nat Med* **5** (7), 803–809.

[24] Vlodavsky I, Elkin M, Pappo O, Aingora H, Atzmon R, Ishai-Michaeli R, Avi A, Pecker I, and Friedmann Y (2000). Mammalian heparanase as mediator of tumor metastasis and angiogenesis. *Isr Med Assoc J* **2,** 37–45.

[25] Vlodavsky I and Friedmann Y (2001). Molecular properties and involvement of heparanase in cancer metastasis and angiogenesis. *J Clin Invest* **108,** 341–347.

[26] Correa M, Machado J Jr, Carneiro CR, Pesquero JB, Bader M, Travassos LR, Chammas R, and Jasiulionis MG (2005). Transient inflammatory response induced by apoptotic cells is an important mediator of melanoma cell engraftment and growth. *Int J Cancer* **114** (3), 356–363.

[27] Rubin H (2001). Selected cell and selective microenvironment in neoplastic development. *Cancer Res* **61,** 799–807.

[28] Rak J, Mitsuhashi Y, Sheehan C, Krestow JK, Florenes VA, Filmus J, and Kerbel RS (1999). Collateral expression of proangiogenic and tumorigenic properties in intestinal epithelial cell variants selected for resistance to anoikis. *Neoplasia* **1** (1), 23–30.

[29] Zhu Z, Sanchez-Sweatman O, Huang X, Wiltrout R, Khokha R, Zhao Q, and Gorelik E (2001). Anoikis and metastatic potential of Cloudman S91 melanoma cells. *Cancer Res* **61,** 1707–1716.

[30] Diaz-Montero CM and McIntyre BW (2003). Acquisition of anoikis resistance in human osteosarcoma cells. *Eur J Cancer* **39** (16), 2395–2402.

[31] Herlyn M, Clark WH, Rodeck U, Mancianti ML, Jambrosic J, and Koprowski H (1987). Biology of tumor progression in human melanocytes. *Lab Invest* **56,** 461–474.

[32] Krengel S, Stark I, Geuchen C, Knoppe B, Scheel G, Schlenke P, Gebert

A, Wunsch L, Brinckmann J, and Tronnier M (2005). Selective down-regulation of the alpha6-integrin subunit in melanocytes by UVB light. *Exp Dermatol* **14** (6), 411−419.

[33] Guo W and Giancotti FG (2004). Integrin signalling during tumour progression. *Nat Rev Mol Cell Biol* **5,** 816−826.

[34] Lewis JM, Truong TN, and Schwartz MA (2002). Integrins regulate the apoptotic response to DNA damage through modulation of p53. *Proc Natl Acad Sci USA* **99** (6), 3627−3632.

[35] Guo HB, Lee I, Kamar M, Akiyama SK, and Pierce M (2002). Aberrant N-glycosylation of β_1 integrin causes reduced $\alpha_5\beta1$ integrin clustering and stimulates cell migration. *Cancer Res* **62**, 6837−6845.

[36] Jasiulionis MG, Chammas R, Ventura AM, Travassos LR, and Brentani RR (1996). Alpha6beta1-integrin, a major cell surface carrier of beta1−6−branched oligosaccharides, mediates migration of EJ-ras−transformed fibroblasts on laminin-1 independently of its glycosylation state. *Cancer Res* **56** (7), 1682−1689.

[37] Guo P, Wang QY, Guo HB, Shen ZH, and Chen HL (2004). *N*-acetyl-glucosaminyltransferase V modifies the signaling pathway of epidermal growth factor receptor. *Cell Mol Life Sci* **61**, 1795−1804.

[38] Murata K, Miyoshi E, Ihara S, Noura S, Kameyama M, Ishikawa O, Doki Y, Yamada T, Ohigashi H, Sasaki Y, et al. (2004). Attachment of human colon cancer cells to vascular endothelium is enhanced by *N*-acetylglucosaminyltransferase V. *Oncology* **66**, 492−501.

[39] Dennis JW, Granovsky M, and Warren CE (1999). Glycoprotein glycosylation and cancer progression. *Biochim Biophys Acta* **1473** (1), 21−34.

[40] Demetriou M, Nabi IR, Coppolino M, Dedhar S, and Dennis JW (1995). Reduced contact-inhibition and substratum adhesion in epithelial cells expressing GlcNAc-transferase V. *J Cell Biol* **130**, 383−392.

[41] Morgan R, Gao G, Pawling J, Dennis JW, Demetriou M, and Li B (2004). *N*-acetylglucosaminyltransferase V (Mgat5)−mediated N-glycosylation negatively regulates Th1 cytokine production by T cells. *J Immunol* **173** (12), 7200−7208.

[42] Chammas R, Veiga SS, Travassos LR, and Brentani RR (1993). Functionally distinct roles for glycosylation of alpha and beta integrin chains in cell−matrix interactions. *Proc Natl Acad Sci USA* **90** (5), 1795−1799.

[43] Bellis SL (2004). Variant glycosylation: an underappreciated regulatory mechanism for beta1 integrins. *Biochim Biophys Acta* **1663** (1−2), 52−60.

[44] Guo HB, Lee I, Kamar M, and Pierce M (2003). *N*-acetylglucosaminyl-transferase V expression levels regulate cadherin-associated homotypic cell−cell adhesion and intracellular signaling pathways. *J Biol Chem* **278** (52), 52412−52424.

[45] Przybylo M, Hoja-Lukowicz D, Litynska A, and Laidler P (2002). Different glycosylation of cadherins from human bladder non-malignant and cancer cell lines. *Cancer Cell Int* **2**, 6−10.

[46] De Souza GA, Godoy LMF, Teixeira VR, Otake AH, Sabino A, Rosa JC, Dinarte AR, Pinheiro DG, Silva WA Jr, Eberlin MN, et al. (2006). Proteomic and SAGE profiling of murine melanoma progression indicates the reduction of proteins responsible for ROS degradation. *Proteomics* **6** (in press).

[47] Sasisekharan R, Shriver Z, Venkataraman G, and Narayanasami U (2002). Roles of heparan-sulfate glycosaminoglycans in cancer. *Nat Rev Cancer* **2**, 521−528.

[48] Liu D, Shriver Z, Venkataraman G, El Shabrawi Y, and Sasikharan R (2002). Tumor cell surface heparin sulfate as cryptic promoters or inhibitors of tumor growth and metastasis. *Proc Natl Acad Sci USA* **99**, 568−573.

[49] Staquicini FI, Moreira CR, Nascimento FD, Tersariol IL, Nader HB, Dietrich CP, and Lopes JD (2003). Enzyme and integrin expression by high and low metastatic melanoma cell lines. *Melanoma Res* **13**, 11−18.

[50] Dietrich CP, Schibuola CT, Sampaio LO, and Ibara I (1978). Changes in the composition of sulfated mucopolysaccharides during neoplastic transformation of cerebral tissue. *Cancer Res* **38**, 3969−3971.

[51] Sharma B, Handler M, Eichstetter I, Whitelock JM, Nugent MA, and Iozzo RV (1998). Antisense targeting of perlecan blocks tumor growth and angiogenesis *in vivo*. *J Clin Invest* **102**, 1599−1608.

[52] Timar J, Lapis K, Dudas J, Sebestyen A, Kopper L, and Kovalszky I (2002). Proteoglycans and tumor progression: Janus-faced molecules with contradictory functions in cancer. *Semin Cancer Biol* **12**, 171−173.

[53] Iozzo RV, Cohen IR, Grassel S, and Murdoch AD (1994). The biology of perlecan: the multifaceted heparan sulfate proteoglycan of basement membranes and pericellular matrices. *Biochem J* **302** (Part 3), 625−639.